ELISE: A Reinforcement Learning Framework to Optimize the Sloftframe Size of the TSCH Protocol in IoT Networks

F. Fernando Jurado-Lasso, *Member, IEEE*, Mohammadreza Barzegaran, *Member, IEEE*, J. F. Jurado, and Xenofon Fafoutis, *Senior Member, IEEE*

***Abstract*—The Internet of Things (IoT) is shaping the next generation of cyber-physical systems to improve the future industry for smart cities. It has created novel and essential applications that require specific network performance to enhance the quality of services. Since network performance requirements are application-oriented, it is of paramount importance to provide tailored solutions that seamlessly manage the network resources and orchestrate the network to satisfy user requirements. In this article, we propose ELISE, a Reinforcement Learning (RL) framework to optimize the slotframe size of the Time Slotted Channel Hopping (TSCH) protocol in IIoT networks while considering the user requirements. We primarily address the problem of designing a framework that self-adapts to the optimal slotframe length that best suits the user's requirements. The framework takes care of all functionalities involved in the correct functioning of the network, while the RL agent instructs the framework with a set of actions to determine the optimal slotframe size each time the user requirements change. We evaluate the performance of ELISE through extensive analysis based on simulations and experimental evaluations on a testbed to demonstrate the efficiency of the proposed approach in adapting network resources at runtime to satisfy user requirements.**

***Index Terms*—Industrial Internet of Things (IIoT), Wireless Sensor Networks (WSNs), Network Management, Reinforcement Learning (RL), Time Slotted Channel Hopping (TSCH).**

I. Introduction

The world has witnessed a shift from traditional communication networks that interconnect computers through well-established standards to a pervasive network of networks that provides internet connectivity even to the smallest physical objects. This evolved communication network, known as the IoT, is the enabling technology for Industry 4.0, where operational technology meets information technology. These cutting-edge technologies have created novel and essential applications for industrial operations such as smart cities, intelligent energy management, transportation, homes, waste management, etc.

At the hardware level, intelligent electronic devices embedded with computing, communication systems, sensors, and actuators realize such applications. This has led to the development of Wireless Sensor Network (WSN) technology, which is flexible, cost-effective, and suitable for embedding into small objects. WSN find applications in various industrial domains [1]–[3], and their architecture is constrained by size, cost, and limited resources such as computation capabilities, energy, memory, and communication bandwidth. Effective management of these resources is crucial to ensure optimal performance over an extended period.

Energy consumption is a crucial performance metric in WSNs. Wireless sensor nodes can reduce energy consumption by periodically turning off their radio chipsets [4]. However, implementing these sleeping periods requires strict scheduling algorithms to coordinate transmission and reception times among neighboring nodes. The IEEE 802.15.4 - Time Slotted Channel Hopping (TSCH) standard provides functionalities for link scheduling in low-rate WSNs [5], [6]. The scheduling algorithm, known as the scheduler, generates cyclic schedules called *slotframes*, determining the physical channel for transmission at each time point. The schedule significantly affects network performance. Redundant links improve reliability and latency but increase power consumption as receiving nodes wake up their radios more frequently. Smaller slotframe sizes enhance network reliability and latency at the expense of higher power consumption, while larger slotframe sizes minimize power consumption but compromise reliability and latency. To meet application needs, the scheduling algorithm must consider user requirements, enabling a tailored schedule that is flexible, adaptable, and reliable, accommodating dynamic changes in the environment and user requirements.

A. Contributions

In this article, we propose an open-source reinforcement learning framework named ELISE[1] to optimize the slotframe

Manuscript received June 7, 2023; revised xx, xx. This work was partly supported by DAIS. DAIS (https://dais-project.eu/) has received funding from the ECSEL Joint Undertaking (JU) under grant agreement No 101007273. The JU receives support from the European Union's Horizon 2020 research and innovation programme and Sweden, Spain, Portugal, Belgium, Germany, Slovenia, Czech Republic, Netherlands, Denmark, Norway, and Turkey. The document reflects only the authors' view, and the Commission is not responsible for any use that may be made of the information it contains. Danish participants are supported by Innovation Fund Denmark under grant agreement No. 0228-00004A.

F. Fernando Jurado-Lasso and Xenofon Fafoutis are with the Embedded Systems Engineering section, DTU Compute, Technical University of Denmark, 2800 Lyngby, Denmark (e-mail: ffjla@dtu.dk; xefa@dtu.dk).

Mohammadreza Barzegaran is with the Center for Pervasive Communication and Computing, University of California, Irvine, CA 92697, USA (e-mail: barzegm1@uci.edu).

J. F. Jurado is with the Department of Basic Science, Faculty of Engineering and Administration, Universidad Nacional de Colombia Sede Palmira, Palmira 763531, Colombia (e-mail: jfjurado@unal.edu.co).

[1]https://github.com/fdojurado/SDWSN-controller.git

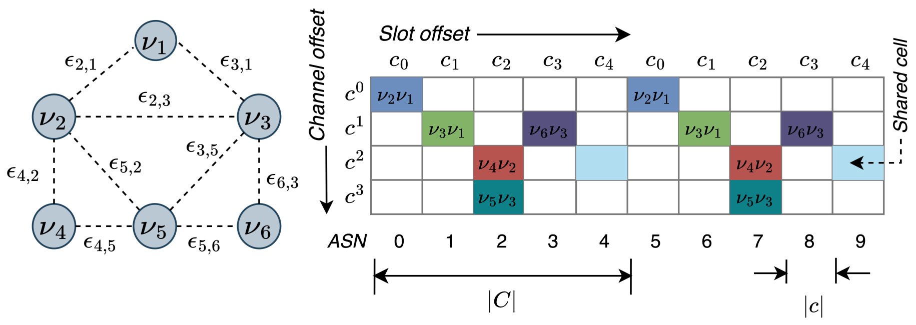

Fig. 1. An example of a TSCH schedule for a six-nodes topology.

size of TSCH networks, considering dynamic changes in user requirements. We address the problem of designing a framework that self-adapts the slotframe size of the TSCH schedule to the optimal length that best suits a set of user requirements. ELISE guides the network through a set of actions to determine the optimal slotframe size whenever user requirements change.

The main contributions of this article are as follows:

1) We develop a novel open-source framework that enables centralized network resource management and run-time reconfiguration of WSNs.
2) We develop a reinforcement learning solution that utilizes the ELISE framework to self-adapt the network's reliability, power efficiency, and delay based on user requirements.
3) We design a reward model based on a multi-objective cost function that facilitates the selection of the best network configuration to meet user requirements.
4) We evaluate the performance of ELISE through extensive analysis using simulations and experimental evaluations on a testbed.

The remainder of this article is organized as follows. Section II provides a technical background on key concepts in the framework and an overview of related research. Section III provides a detailed description of the framework components. Section IV explains the design of the reinforcement learning framework. Section V presents the experimental layout, the approximation model, the training process, and the experimental evaluation. Finally, Section VI presents the main conclusions and potential areas for future research.

II. Background and Related Work

In this section, we briefly introduce the network model and the core technologies used throughout this paper: TSCH and Software-Defined Wireless Sensor Networks (SDWSNs). We then discuss research works that have used these technologies to improve network performance.

A. Network model

We model the network as a directed graph $G(\mathcal{V},\mathcal{E})$, where $\mathcal{V}$ is the set of nodes, and $\mathcal{E}$ is the set of physical links. A node $\nu_i \in \mathcal{V}$ is the sender and/or receiver of network traffic. The number of network nodes is denoted with $|\mathcal{V}|$. A link $\epsilon_{i,j} \in \mathcal{E}$ is a full-duplex link that connects the two nodes ν_i and ν_j. since the links are bi-directional, the link $\epsilon_{i,j}$ is equivalent to $\epsilon_{j,i}$. The number of network links is denoted with $|\mathcal{E}|$.

The network traffic is modeled with the concept of streams (also called flows) that represents a data packet from one sender (talker) to one or multiple receivers (listeners). We denote the set of network streams as $\mathcal{T}$. A stream $\tau_i \in \mathcal{T}$ is characterized by the talker and the receiver. In ELISE, we limit the number of listeners for each stream to one, i.e., unicast communication. However, the model can be easily extended to support multicast streams by adding each sender-receiver pair as a stream.

The path for the stream τ_i is determined as an ordered sequence of directed links and denoted with $r_i \in R$. Besides, $|r_i|$ represents the number of links in the path. For example, the stream $\tau_1 \in \mathcal{T}$ sending from the node ν_1 to the node ν_3 has the route $r_1 = \{\epsilon_{1,2}, \epsilon_{2,5}, \epsilon_{5,3}\}$. Using the set of routes R, we define the function $\mathcal{H} : \nu_i \longrightarrow \mathbb{N}$ which takes the node ν_i as the input and returns the node rank, i.e., the number of links originated for the node ν_i, as the output. Fig. 1 presents an example of a TSCH schedule for six-node network topology.

B. SDWSNs

We model the network as a Software-Defined Wireless Sensor Network (SDWSN). This architecture adopts concepts from Software-Defined Networking (SDN) which divides the control from the data functions, allowing the logically centralized controller to become reprogrammable and the WSN to be abstracted for applications and network services [7]. SDN separates the network into three network planes: application, control, and data plane. The application plane hosts applications and programs that send information about the network requirements to the SDN controller. In contrast, the control plane is a logically centralized entity that processes application requirements and sets up the network infrastructure resources to satisfy them. Lastly, the data plane is the network infrastructure with little intelligence that follows orders from the control plane. Readers interested in a thorough background, challenges, and benefits of SDWSNs can refer to [7]–[9].

C. Orchestra

Orchestra [10] is designed to run multiple stacked slotframes that repeat at different periods to ensure they do not interfere evenly. Each slotframe is allocated to a specific network plane that is defined by SDWSN. The scheduler selects the slotframe with higher priority to run when multiple slotframes need the communication medium simultaneously. In its default configuration, Orchestra runs three slotframes: i) Enhanced Beacon (EB), ii) unicast, and iii) default traffic slotframes. The EB slotframe is a communication link from sensor nodes to its children to set the time source. The unicast slotframe contains links to every neighbor in the WSN. The default slotframe is used for traffic other than EB and unicast packets.

D. TSCH

TSCH is a globally synchronized network where traffic is transmitted based on a static cyclic schedule table called slotframe C that repeats with the period equal to the slotframe size $|C|$ [11], [12]. In a TSCH network, the slotframe (schedule) is divided into equal-length timeslots as shown in Fig. 1. We denote each timeslot with $c_j \in C$ and its length with $|c|$ (same length for all timeslots). The timeslot length $|c|$, typically 10 ms, is long enough for the transmission and acknowledgment of frames.

To this end, the slotframe size C is equal to the size of n timeslots, denoted with $|C| = n \times |c|$. Within a slotframe, timeslots are counted with their subscripts j. Similarly, the timeslots can be counted from when the network booted with an Absolute Slot Number (ASN). The ASN serves as a global clock, and it increases at every timeslot.

Each timeslot c_j is divided into a fixed number of cells. Each cell denoted with c_j^k indicates the channel offset k. For channel hopping a cell is used to find the physical channel to transmit. Considering an array of channel frequencies F to hop over, the channel frequency f for the cell c_j^k is calculated in Eq. (1).

$$f = F[(j + k)\%|F|] \tag{1}$$

To this end, each cell will select a different physical channel at consecutive slotframes. The scheduler oversees the role of cells in the slotframe. The roles can be shared, dedicated, or empty cells. Shared cells (light blue cells in the example) are contention-based. They are used by multiple transmitters, increasing the probability of interference as they can transmit simultaneously. Reliable transmissions resend frames using a back-off window when no acknowledgment is received. Dedicated cells (cells labeled with a pair of nodes) are contention-free. They are allocated carefully not to cause interference issues with other cells. Retransmissions can occur due to external interference or bad radio link quality [13].

The example provides an illustration of a TSCH schedule that has been designed for a six-node WSN. The slotframe size is five timeslots $n = 5$. There are six cells with a non-empty role, one shared cell shown with c_4^2. There are five dedicated cells that permit the communication of nodes with their parents. There are also two non-interfering transmissions at the same slot offset (c_2^2, c_2^3).

E. Related work

Table I presents a summary of the latest research works on related topics including TSCH, SDWSNs, and RL. It also provides information related to the year of conception, whether the given article considers user requirements, and major contributions. Research works [15], [16] strive to improve the network performance using SDWSNs. The centralized architecture of SDWSNs allows the control plane to build a global view of the network that permits it to make better decisions, in this case, to provide support for mobile sensor nodes. The research work in [15] uses a static TSCH schedule with redundant links for mobile nodes to improve reliability, whereas [16] uses a supervised learning approach to separate mobile from static nodes. Articles [17], [18] oversee the IoT network through the centralized controller, which enables the collection of observations to design, implement and train a learning agent to maximize the accumulative reward of actions taken. The work in [17] focuses on monitoring the SDWSN traffic, at granularity levels to mitigate flow-table overflows, while [18] uses a learning agent to find the optimal forwarding paths for the SDWSN. Articles [10], [13] aim to improve the performance of TSCH networks. Research work [13] objective is to reduce the packet latency. This is achieved by dividing the slotframe into small chunks. Sensor nodes select the chunk to transmit based on their distance to the border router to minimize the latency. The work in [10], which has been previously introduced, is an autonomous scheduler with little overhead that provides high reliability. The article in [14] main objective is to select among a set of routing algorithms the best that suits the given user requirements. The selection of the routing algorithm is achieved using a supervised learning approach. The research work in [19] presents a RL approach to configure the Carrier-Sense Multiple Access/Collision Avoidance (CSMA/CA) parameters in a multi-hop TSCH network. The framework utilizes neural networks to converge to Quality of Service (QoS) satisfying configurations efficiently.

Overall, these studies aim to enhance the QoS in network applications. Performance metrics such as energy, delay, and reliability are considered, but there has been limited attention given to real user needs. It is crucial to provide a customized engineering solution that seamlessly manages network resources and orchestrates the network to meet the specific requirements of applications or users. However, as observed from the table, this aspect has not received significant focus. While the work presented in [14] takes user requirements into account in their proposed approach, their supervised learning method encounters challenges in predicting the optimal routing algorithm in dynamic environments like WSNs. Furthermore, they do not consider the MAC layer, which is responsible for the duty cycle of sensor nodes in state-of-the-art WSNs, directly impacting power consumption, delay, and reliability.

III. ELISE Framework architecture overview

This section presents an overview of the ELISE functional framework and architecture. Next, a detailed description of their components is presented, such as the layered architecture planes.

TABLE I
SUMMARY OF RELATED WORKS.

Article	Year	Topic			UR	Major contribution(s)
		TSCH	SDWSNs	RL		
[10]	2015	✓	✗	✗	✗	Autonomous scheduler for TSCH without control overhead that does not rely on centralized or distributed entities.
[14]	2017	✗	✓	✗	✓	A decision-making approach to select the routing protocol that best suits the application requirements to get optimal performance using supervised learning.
[15]	2020	✓	✓	✗	✗	An SDN-based network architecture that provides support to mobile nodes using TSCH. Mobile nodes have one up- and down-link to every node in the network regardless of their position in the WSN.
[16]	2020	✗	✓	✗	✗	An SDN-based approach to pinpoint mobile nodes in WSNs. The approach features a mobility detector and a k-means cluster algorithm to decouple static from mobile nodes.
[13]	2020	✓	✗	✗	✗	A low-latency distributed scheduling function to optimize the End-to-End delay, and reliability.
[17]	2021	✗	✓	✓	✗	A traffic monitoring framework for SDWSNs. They trained a double deep Q-network (DDQN) agent to achieve the optimal flow rule match-field policy.
[18]	2021	✗	✓	✓	✗	A reinforcement learning approach to select the best routing path that improves the QoS of the SDWSN.
[19]	2023	✓	✗	✓	✓	A reinforcement learning approach to configure the parameters of the CSMA/CA of the TSCH protocol to achieve distinctive QoS.
ELISE	2023	✓	✓	✓	✓	An open-source framework that self-configures network resources in run-time to satisfy the dynamic user requirements for SDN-based IoT networks.

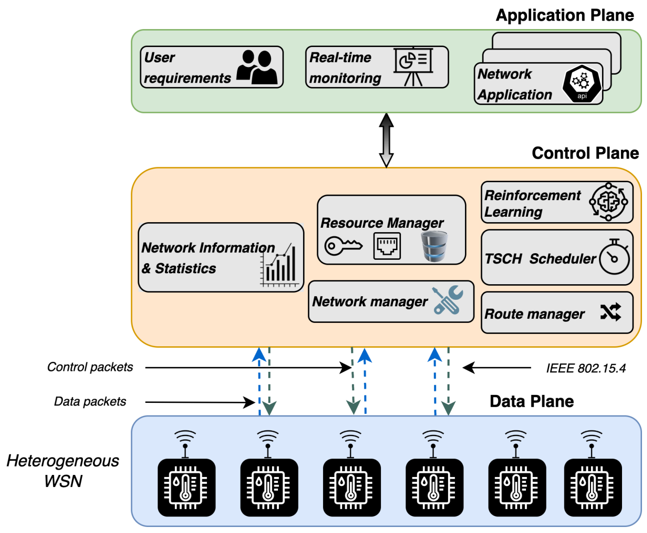

Fig. 2. ELISE architecture.

A high-level overview of the ELISE framework architectural structure, including its main components and interfaces, is shown in Fig. 2. The architectural structure follows the typical three-tier SDN principles for WSNs. The description of each layer of the architecture from the bottom-up is as follows.

A. Data plane

The data plane is built upon the interconnection of multiple wireless sensor nodes, for simplicity we call them sensors. In ELISE, we have defined two types of sensors: the (regular) sensor node and the sink. All sensor nodes, including the sink, communicate with each other using IEEE 802.15.4 radios; however, the sink is also directly connected to the control plane through a wired interface. All sensor nodes of the network graph that are denoted with $\nu \in \mathcal{V}$ and all radio communication links are denoted with $\epsilon \in \mathcal{E}$, see Sect. II-A for more information. Besides, we assume that sensor nodes

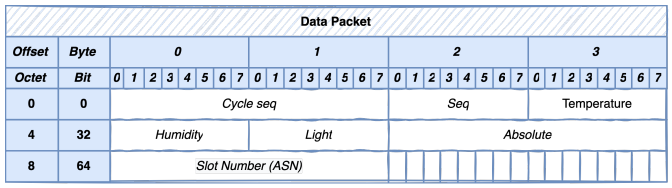

Data Packet					
Offset	Byte	0	1	2	3
Octet	Bit	0 1 2 3 4 5 6 7	0 1 2 3 4 5 6 7	0 1 2 3 4 5 6 7	0 1 2 3 4 5 6 7
0	0	Cycle seq		Seq	Temperature
4	32	Humidity	Light	Absolute	
8	64	Slot Number (ASN)			

Fig. 3. Data packet format.

are the talkers of network streams and all streams have the same listener node, i.e., the sink or the controller node.

Overall the entire network infrastructure runs on a lightweight embedded operating system. Among the available embedded operating systems in the market [7], we have selected Contiki-NG [20] because (i) it is open-source, well documented, and it has a large community, (ii) it is widely used in the research community, (iii) it provides the implementation of TSCH and Orchestra, (iv) it can run on both Cooja network simulator [21] and real hardware. To comply with SDWSN principles of making the network infrastructure run simple tasks and remove energy-intensive functions from sensor nodes, we have redesigned the protocol stack, from layers three and up, to support the following five functionalities.

1) Data packets: The packet format is shown in Fig. 3. The cycle sequence and sequence fields are used, by the reinforcement learning algorithm, to keep track of the number of packets received in the corresponding cycle. Temperature, humidity, and light are physical variables measured by sensors (this can be generalized to variables one, two, and three). The ASN field contains the ASN when the packet was created. This field is useful to calculate the packet latency under specific network configurations such as routes, TSCH schedules, etc.

2) Neighbor discovery (ND): This packet discovers other sensor devices in the sender transmission range. It also allows discovering neighbors with paths to the controller. This packet contains three fields: rank, Received Signal Strength Indicator (RSSI), and checksum. The rank field is equivalent to $\mathcal{H}$ which

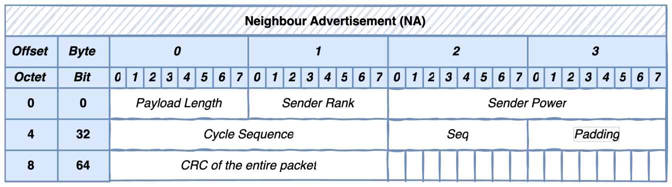

Neighbour Advertisement (NA)

Offset	Byte	0	1	2	3
Octet	Bit	0 1 2 3 4 5 6 7	0 1 2 3 4 5 6 7	0 1 2 3 4 5 6 7	0 1 2 3 4 5 6 7
0	0	Payload Length	Sender Rank	Sender Power	
4	32	Cycle Sequence		Seq	Padding
8	64	CRC of the entire packet			

Fig. 4. Neighbor advertisement header format.

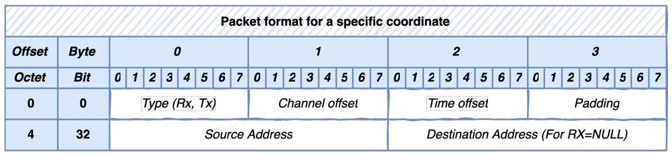

Packet format for a specific coordinate

Offset	Byte	0	1	2	3
Octet	Bit	0 1 2 3 4 5 6 7	0 1 2 3 4 5 6 7	0 1 2 3 4 5 6 7	0 1 2 3 4 5 6 7
0	0	Type (Rx, Tx)	Channel offset	Time offset	Padding
4	32	Source Address		Destination Address (For RX=NULL)	

Fig. 5. Packet format of a TSCH schedule link.

is the number of links originated from the talker node (see Sect. II-A). The RSSI field specifies the accumulative RSSI to the controller. This field permits the receiver node to decide which parent to choose between two equal rank values. Lastly, the checksum field is an error checking of the packet integrity.

3) Neighbor advertisement (NA): This packet contains messages to report their status and neighbors' to the controller, including the average power consumption, rank, and links to neighbors. The format of the packet header is shown in Fig. 4. The payload length field states the number of bytes contained in the packet payload. The sender rank specifies the rank of the sender. The sender power field contains the power consumption of the sender. Cycle sequence and sequence fields fulfill the same function as in the data packet. The CRC field is an error checking of the packet integrity. The payload consists of neighbors' addresses, RSSI, and Link Quality (LQ) values.

4) Network configuration - TSCH schedules: This packet type is a control message to establish the TSCH schedules for the incoming cycle. The header has four fields: payload length, slotframe size $|C|$, sequence, and CRC. The payload length, sequence, and CRC fields fulfill the same functions mentioned above. The slotframe size field contains the length of the schedules encapsulated in the payload. The format of a TSCH link embedded in the payload of this control packet is shown in Fig. 5. The type field states the type of TSCH link: transmit (Tx) or listen (Rx). The channel and time offset fields specify the coordinates of the given link. The source address field indicates the address of the sensor node that needs to process this link. Lastly, the destination address is used for Tx link types to set the neighbor address.

5) Network configuration - Routes: This packet type is also a control message to establish the forwarding paths for the incoming cycle. The packet header consists of payload length, sequence, and CRC fields which fulfill the same function mentioned above. The packet payload contains the source, destination, and neighbor addresses to build the forwarding paths.

Control packets including TSCH schedules, and route packets are broadcasted into the WSN. ELISE defines four slotframes, inspired by Orchestra, for specific traffic planes: EB slotframe for the time source, control traffic slotframe for control packets, data traffic slotframe for data packets, and the default traffic slotframe for any other type of traffic. The control traffic is a broadcast slotframe that permits the transmission and reception of new TSCH schedules and route configurations.

For cell c_j^k, the time slot number j and channel offset k for sensor node ν_i and control plane slotframe size of $|C|$ are calculated as follows.

$$j = \mathcal{H}(\nu_i)\%|C| \tag{2}$$

$$k = ((i)\%|C| - 1) + 1 \tag{3}$$

These two equations minimize communication interference between sensor nodes with equal rank values that try to broadcast control packets to their children.

B. Control plane

The control plane can run locally on a computer or in the cloud. At its core, it is implemented in Python 3 [22] because it supports multiple machine learning libraries available in the market, has a large community, and has an ample library collection. Here, we briefly introduce the core functionalities of each module.

1) Network information and statistics: This module holds all network information collected. It also includes all packets received and simple statistics.

2) Resource manager: This module is in charge of orchestrating all resources in the control plane. Resources in this module include database, serial interface, and network access.

3) Network manager: This module holds key functions to correctly operate the data plane. Functions such as writing and reading from the network reside here.

4) Route manager: This module hosts all functionalities to build the forwarding paths of the network. It hosts multiple traditional routing algorithms. It is also flexible to allow adding new centralized routing protocols.

5) TSCH manager: In this module resides the functions to correctly build TSCH schedules. It has been designed to easily create new TSCH schedulers on top.

6) Reinforcement learning: The reinforcement learning module is the main intelligent component of the entire control plane. It uses all other modules to collect data, learn from the environment, tune hyper-parameters and evaluate the trained agent. This module is discussed in detail in the next section.

C. Application plane

The application plane hosts user requirements and programs such as real-time monitoring tools that convey information regarding the status of the network. This plane instructs the control plane on the current user requirements through the northbound API.

IV. Reinforcement Learning Module

This section takes the reader through the design and implementation of a reinforcement learning approach to optimize the slotframe size of TSCH in SDN-based IoT networks

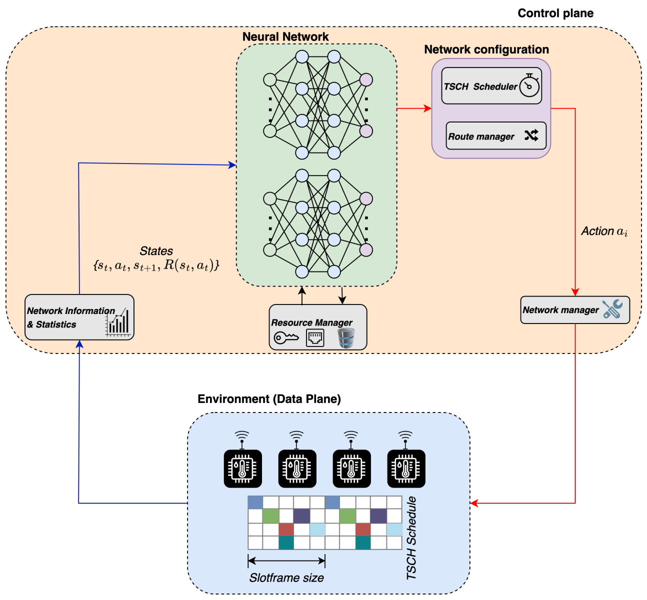

Fig. 6. The architecture of the RL agent of ELISE.

considering the user requirements. Readers interested in the background of RL can refer to [23] and its applications to SDWSNs can be found in [7].

A. Solution approach

To solve this multi-objective function that self-adapts the slotframe size of the TSCH schedule to the optimal length that best suits a set of user requirements, we use a reinforcement learning agent that hosts neural networks in its core, as shown in Fig. 6. ELISE provides flexibility to evaluate different reinforcement learning algorithms. Algorithms that we consider in this research are Deep Q Network (DQN) [17], Asynchronous Advantage Actor Critic (A2C) [24], and Proximal Policy Optimization (PPO) [25].

The proposed solution follows the typical three-tier principles for SDWSNs, where the control plane layer collects data, orchestrates resources, performs intelligent calculations, and deploys new network configurations into sensor nodes. At the initial state of the data plane, sensor nodes discover their path to the controller using ND packets. They then start sending NA packets to the controller. The controller processes these packets to make future decisions. The reinforcement learning agent predicts the next slotframe size. It then prepares the TSCH schedules and routes using the TSCH and route manager module. Finally, the control plane deploys new configurations through the network management module.

ELISE develops a Markov Decision Process (MDP) framework with the architecture depicted in Fig. 6. This framework enables the reinforcement learning algorithm to dynamically select and deploy optimal actions based on the observations to maximize the average accumulative reward. The MDP is represented by a tuple $<\mathcal{S}, \mathcal{A}, \mathcal{R}>$, where $\mathcal{S}$ represents the state space, $\mathcal{A}$ represents the action space, and $\mathcal{R}$ represents the immediate reward.

- State Space: As previously discussed, there are three performance metrics, and three user requirements, at the end of each iteration. However, the learning time can be reduced by adding the last scheduled link in the TSCH slotframe (λ), and the current slotframe size ($|C|$). λ enables the agent to avoid slotframe sizes that are below the last scheduled link in the scheduler, otherwise, it can alter the normal behavior of the TSCH network. The state space of the proposed work is defined as follows.
$$\mathcal{S} \triangleq \{(\Omega_1, \alpha_1, \beta_1, \gamma_1, \lambda_1, |C|_1), ..., \\ (\Omega_n, \alpha_n, \beta_n, \gamma_n, \lambda_n, |C|_n)\} \tag{4}$$
Where Ω represents the cost of the SDWSN. α, β, and γ are the user-defined coefficients for power consumption, delay, and reliability, respectively.
- Action Space: The RL agent aims to find the optimal slotframe size of the data plane traffic plane given the set of user requirements. At every decision-making point, the agent predicts the next slotframe size given the above-mentioned observations. The agent can take multiple consecutive actions (slotframe sizes) before reaching the optimal solution. The number of steps taken to reach the optimal solution depends on the current state of the environment, especially, the current slotframe size ($|C|$) and the user requirements (α, β, γ).
The agent selects the next action between
  1) increasing $|C|$,
  2) decreasing $|C|$, or
  3) continuing using the current $|C|$.

  The selection of the slotframe size is bounded by numbers that are mutually prime to other slotframes in the TSCH network. Recall that the TSCH network runs multiple stacked slotframes that repeat at different periods (mutually prime slotframe sizes) to ensure they do not interfere evenly. Therefore, the action space for selecting the next slotframe size in the control plane is defined as follows.
$$\mathcal{A} \triangleq \{a : gcd(a, |C|^{EB}, |C|^{CP}, |C|^{DF}) = 1\} \tag{5}$$
Where gcd represents the greatest common divisor, and $|C|^{EB}$,$|C|^{CP}$, and $|C|^{DF}$ are the slotframe sizes of the EB, control, and default traffic planes.
- Immediate reward function: The reward function has been designed to select slotframe sizes within a valid range and to ease learning. Whenever the agent selects a slotframe size below λ, it is penalized. In the other case, whenever the agent selects a slotframe size that goes beyond the maximum valid slotframe size (μ), it is also penalized. The agent learns to select the next action within this valid range while maximizing the accumulative reward. The agent is positively rewarded if the slotframe size lies within the valid range. The amount rewarded depends on the performance metrics and user requirements. The reward function is expressed as follows.
$$\mathcal{R}(s,a) = \begin{cases} -\mathcal{G}_{max}, & |C|^{DP} \geq \mu \\ & |C|^{DP} \leq \lambda \\ \Upsilon - \Omega, & \lambda < |C|^{DP} < \mu \end{cases} \tag{6}$$

Where $|C|^{DP}$ is the slotframe size of the data traffic slotframe, and $\mathcal{G}_{max}$ is the maximum penalty for taking an invalid slotframe size. Υ is a constant that makes sure the immediate reward stays always positive. Υ is equal to the worst case of Ω. Therefore, $\Upsilon = 2$. It is noteworthy that we changed the signs in (7) to maximize the immediate reward function. Also, we have defined two terminating conditions for episodes. We end an episode either every time the agent selects a slotframe size outside the valid range or when we reach the maximum number of timesteps.

B. Cost Function

This reinforcement learning-based model optimizes the slotframe size of the data plane slotframe introduced in the above sections. Other slotframes are not considered in the optimization because they are control slotframes that are mandatory for the basic operation of the network, and tempering with them can make the network fail.

We design a weight-based multi-objective function that captures the cost of the TSCH schedule and the routing. This multi-objective cost function can be expressed as follows.

$$\begin{aligned}&\Omega = \omega_1 \times \omega_2\\&\omega_1 = \alpha \times \widetilde{P} + \beta \times \widetilde{D} + \widetilde{R} \times (1-\gamma)\\&\text{subject to } \alpha + \beta + \gamma = 1.\end{aligned} \tag{7}$$

Where ω_1 captures the cost of scheduling and ω_2 captures the cost of routing, both presented in Sect. IV-C. For the cost of scheduling, α, β, and γ are the user requirements for power consumption, delay, and reliability, respectively. ELISE calculates the performance metrics at the end of every cycle; therefore, the samples within the time interval are considered a constraint (they are strictly greater than zero). This holds for all performance metrics samples. The slot duration of TSCH networks can not be less or equal to zero. It is worth mentioning that the optimization is done over the slotframe size of the data plane slotframe of the TSCH protocol. Therefore, the SDN control plane takes several sequential actions at each network state to find the optimal slotframe size given the user requirements and current network state.

C. Objectives

This section gives the details of the terms of the cost function Ω that captures the network performance. The performance metrics are as follows: power consumption, delay, reliability, and dependability. The first three metrics are used in the cost term ω_1 and the dependability is defined with ω_2.

1) Power consumption: In TSCH networks, nodes wake up their radios at specific timeslots to either transmit a packet or listen to the wireless medium, then switch to another state such as low power mode. In ELISE, we assume three states for a network node: i) listening, ii) transmitting, iii) listening and transmitting (forwarding). We ignore the idle state of the nodes since we aim at minimizing the workload of the network nodes.

The power consumed for transmitting the network stream $\tau_i \in \mathcal{T}$ from the talker to the listener denoted with P_i is calculated from Eq. (8). The consumed power is normalized in the range $[0, 1]$.

$$P_i = \frac{\sum_{\epsilon_{m,n} \in r_i} (V^m \times I^m_{tx} + V^n \times I^n_{rx}) \times |c|}{(V^m \times I^m_{max} + V^n \times I^n_{max}) \times |C|} \tag{8}$$

where V^i is the power supply voltage of the node ν_i (in volts), I^i_{tx} is the transmission current consumption of the node ν_i and I^i_{rx} is the reception current consumption of the node ν_i (both in mA). The maximum value of the current consumption while transmitting and receiving is captured by I_{max}. The average power consumption of the network $\widetilde{P}$ is defined as the average of the power consumed for transmitting all network streams. The controller receives the NA packets from network nodes and processes the data in the sender power fields of the packets and stores them in the database. When a cycle finishes, the controller retrieves, from the database, the latest power consumption, and calculates the network power consumption cost $\overline{P}$ using Eq. (9).

$$\begin{aligned}\widetilde{P}(\theta_1) &= \bar{P} + \theta_1 \times \sigma_P\\ \bar{P} &= \frac{1}{|\mathcal{T}|}\sum_{\tau_i \in T} P_i\\ \sigma_P &= \sqrt{\frac{\sum_{\tau_i \in T} |P_i - \bar{P}|}{|\mathcal{T}|}}\end{aligned} \tag{9}$$

where $\bar{P}$ is the average power consumption in the network, σ_P is the normal distribution of the node power consumption in the network, and θ_1 is the weight of the node power consumption distribution. The larger θ_1 value drives the search for a solution with evenly distributed power consumption across the nodes. With θ_1, the user achieves the desired distribution based on the requirements.

2) Delay: The packet delay is calculated as the interval from when the packet is generated at the talker to when the packet is received by the listener in the control plane. For a TSCH network, we can estimate the packet delay of the stream τ_i using the ASN as follows. The packet delay value is normalized in the range of $[0, 1]$.

$$D_i = (ASN_{tx} - ASN_{rx}) \times \frac{|c|}{|C|} \tag{10}$$

The control plane then calculates the average delay of the network $\widetilde{D}$ using Eq. (11) at the end of each cycle. The controller retrieves from the database, the latest $\bar{D}$ for all network streams $\tau_i \in \mathcal{T}$.

$$\begin{aligned}\widetilde{D}(\theta_2) &= \bar{D} + \theta_2 \times \sigma_D\\ \bar{D} &= \frac{1}{|\mathcal{T}|}\sum_{\tau_i \in T} D_i\\ \sigma_D &= \sqrt{\frac{\sum_{\tau_i \in T} |D_i - \bar{D}|}{|\mathcal{T}|}}\end{aligned} \tag{11}$$

where σ_D captures the normal distribution of stream delays. Using θ_2 user can adjust the weight of delay distribution in calculating the average delay. The larger weight drives the search for a solution with evenly distributed stream delays. Similar to θ_1, the user achieves the desired distribution using θ_2 set.

3) Reliability: To calculate the reliability, we first define the Packet Delivery Ratio (PDR) during a cycle in Eq. (12). The control plane performs the calculation of the PDR as follows.

$$PDR = \frac{|\tau_{rx}|}{|\tau_{tx}|} \quad \text{subject to } \tau_{tx} > 0. \tag{12}$$

where τ_{rx} and τ_{tx} are the numbers of received and transmitted packets, respectively. The control plane queries the database to obtain the latest PDR values in the network and calculates the network reliability $\widetilde{R}$ at every end of a cycle as follows.

$$\widetilde{R} = \frac{1}{PDR} \quad \text{subject to } PDR > 0. \tag{13}$$

4) Dependability: We define the dependability metric ω_2 as the cost function for finding the best path for the streams in the network. The dependability metric is based on a simple concept, i.e., the network is more dependable where fewer nodes are involved in the network functioning (stream transmission). Based on this concept, the most dependable network is the one where all streams use the shortest path for transmission.

To this end, we define the power dependability $PDEP$ of the node $\nu_i \in \mathcal{V}$ in Eq. (14). The power dependability of a node shows how much the node is under the workload, i.e., transmission and receiving the data. The more a node is under the workload, the less dependable is the node.

$$\begin{aligned} &DEP_i = DEP_i^{tx} + DEP_i^{rx} \\ &DEP_i^{tx} = \sum (V^i \times I^i_{tx} \times |c|) \\ &\text{subject to } \forall \epsilon_{i,x} \in r_y \text{ and } \forall r_y \in R, \\ &DEP_i^{rx} = \sum (V^i \times I^i_{rx} \times |c|) \\ &\text{subject to } \forall \epsilon_{z,i} \in r_w \text{ and } \forall r_w \in R \end{aligned} \tag{14}$$

The power dependability of the node represents the workload of the node which is used for determining the most dependable path for a specific stream. Thus, we calculate the dependability of the stream $\tau_j \in \mathcal{T}$ as follows.

$$DEP_j = \prod PDEP_i \quad \text{subject to } \epsilon_{i,x} \in r_j. \tag{15}$$

With the dependability of the streams in the network, we calculate the average dependability of the network ω_2 using Eq. (16).

$$\omega_2 = \frac{1}{|\mathcal{T}|} \sum_{\tau_j \in T} DEP_j \quad \text{subject to } |\mathcal{T}| > 0. \tag{16}$$

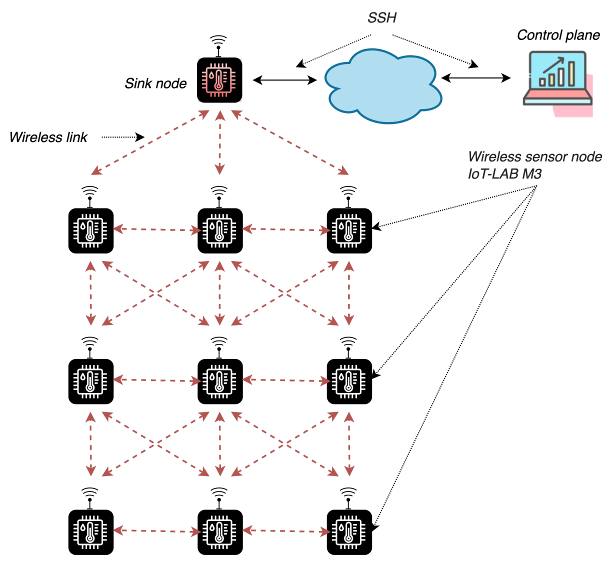

Fig. 7. Topology of the testbed setup.

V. Performance Evaluation

In this section, ELISE's ability to adapt network resources to meet dynamic user requirements is tested. Multiple user requirements are evaluated to understand their impact on performance metrics. We compare ELISE's performance against Orchestra, the preferred TSCH scheduler for IoT networks. The experiments are conducted in both the Contiki Cooja network simulator and a real-world testbed. Due to space limitations, simulation results confirming the findings from the testbed experiments are omitted.

A. Testbed setup

The experiments were conducted at the FIT IoT Lab [26], using a 10-sensor-node network with a maximum depth of three hops. The topology is shown in Fig. 7. The network utilized the IoT-LAB M3 platform, consisting of ARM-Cortex M3 microcontrollers, ATMEL radios, and four sensors. The network run on Contiki-NG, with a redesigned network stack to support SDWSN functionalities. The control plane communicated with the data plane through the Secure Shell Protocol (SSH) and was implemented in Python 3.10 using Stable Baselines 3 [27] for reinforcement learning. The experiment parameters are summarized in Table II. There exist a trade-off between the iteration window interval. A large interval filters out noise but hampers dynamic changes, while a small interval increases noise and network reconfigurations. In our experiments we set this value to 60 control packets ($|\mathcal{T}|$ = 60); however, this value can be changed to meet user requirements. Although with θ_1 and θ_2 in objective metrics (see Sect. IV-C) the desired distribution of power and delay is achievable, for the evaluation where we have considered a fixed path for streams, we set both θ_1 and θ_2 to zero which remove the effect of power and delay distribution in the search. In future work, ELISE will determine the path for streams.

Before we jump into the evaluation of ELISE, we want to discuss in the next section the challenges found while training the reinforcement learning agent.

TABLE II
EXPERIMENT PARAMETERS.

Parameter	Value
No. of sensor nodes ($\|\mathcal{V}\|$)	10
Sensor nodes type	IoT-LAB M3
Transmission power	-17dbm
Iteration window interval	60pkts
Power measure sample time (t_{sample})	60s
Sensor node supply voltage (V)	3V
Network node rank ($\mathcal{H}$)	3
TSCH slot duration ($\|c\|$)	10ms
Reward constant Υ	2
Minimum slotframe size λ	10
Maximum slotframe size μ	70
Penalty $\mathcal{G}_{max}$	-4
Max. episode length ($\mathcal{V}$)	50

B. SDWSN model approximation

The SDWSN model approximation is used to estimate network performance metrics, such as average power consumption, average delay, and network reliability, based on the slotframe size in the TSCH network. This approximation model significantly reduces the iteration time required for training. The values of the performance metrics are estimated using the minimum mean square error (MMSE) estimator. The estimation is performed by sending TSCH schedules with different slotframe sizes and observing the resulting values. The estimated metrics are then used to calculate the immediate reward for actions taken. The approximation model is also used for hyperparameter tuning. The experimental setup and parameters are described, and the estimated values of the performance metrics against the slotframe size are plotted in Fig. 8. The results show that average power consumption decreases exponentially, while average delay increases linearly with the slotframe size. Network reliability decreases linearly but at a smaller rate. This approximation model is used to train and test the DQN, A2C, and PPO algorithms in the testbed.

C. Training

We train the agents over $100k$ iterations. We omit the training figure due to space constraints. However, PPO seems to be the best candidate to solve the problem. However, we also evaluate the algorithms' performance by taking solely deterministic actions over 100 episodes to decide on which algorithm to pick. Table III shows that PPO obtained the greatest average accumulative reward followed by A2C and DQN. Therefore, we use PPO for our result analysis in the testbed. We also tune the hyperparameters of the PPO model. For hyperparameter tuning, we used Optuna [28] which is a hyperparameter optimization framework for machine learning. We tune the hyperparameters for PPO using a random sampler and medium pruner, eight parallel jobs, with 1000 trials and a maximum of 50000 steps.

D. Experimental evaluation

We evaluate the ELISE framework and the trained agent in the real-world testbed. The agent takes deterministic actions and is tested in a scenario with four distinct user requirements:

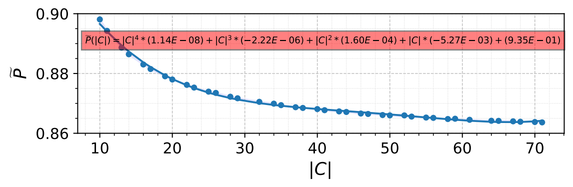

(a) Normalized average network power consumption over slotframe size.

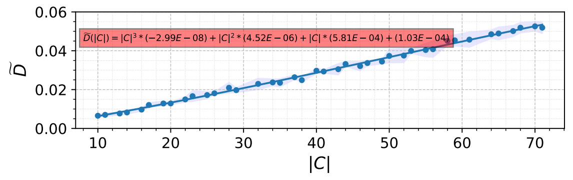

(b) Normalized average network delay over slotframe size.

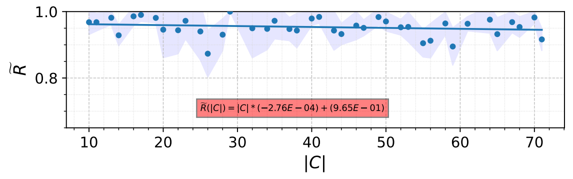

(c) Normalized average network reliability over slotframe size.

Fig. 8. Experimental $\widetilde{P}$, $\widetilde{D}$, and $\widetilde{R}$ values for different slotframe sizes $|C|$.

TABLE III
EVALUATION OF DQN, A2C, AND PPO ALGORITHMS OVER 100 EPISODES.

Algorithm	Avg. Accumulative Reward
PPO	56.44 ± 0.11
A2C	56.37 ± 0.14
DQN	56.34 ± 0.15

balanced, prioritized delay, prioritized power consumption, and prioritized reliability. This scenario allows us to assess the agent's ability to select the best action based on observations and changing user requirements. The evaluation consists of 10 episodes, each lasting for 160 iterations. Each iteration, representing the window interval, takes approximately four minutes. Therefore, each episode runs for around 10.6 hours. The initial slotframe size is set to 10 for all episodes. Results are plotted for each performance metric and the immediate reward against the slotframe size using the 95% confidence interval. The experimental results are shown in Fig 9.

1) Balanced SDWSN: Considering a balanced requirement where equal priority is given to all three performance metrics, we set the user coefficients α, β, and γ to 0.4, 0.3, and 0.3, respectively. This requirement is applied from timestep zero to timestep 40 (Zone 1 in Fig.9). The trained agent takes an average of three actions to reach a steady state slotframe size ($|C|$) of 18, effectively balancing all performance metrics. The average power consumption is approximately 4443μW (Fig.9a), the average delay is around 220ms (Fig.9b), and the average reliability is about 0.95 (Fig.9c). The network reliability exhibits a larger distribution due to interference sources

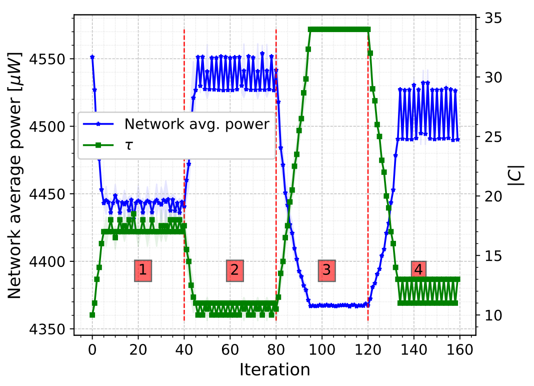

(a) Network average power consumption over the number of iterations.

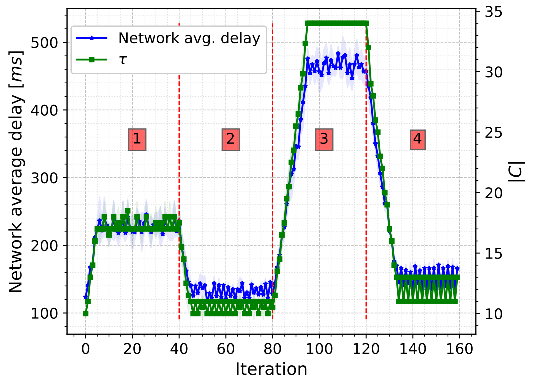

(b) Network average delay over the number of iterations.

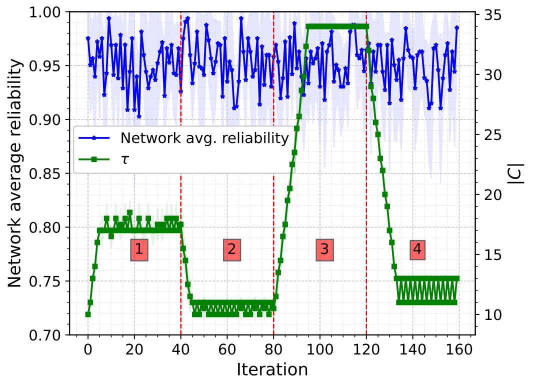

(c) Network average reliability over the number of iterations.

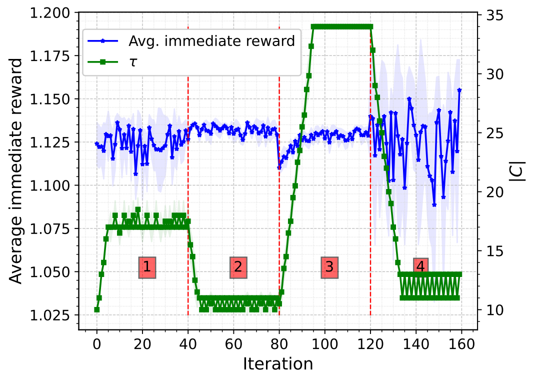

(d) Network average immediate reward over the number of iterations.

Fig. 9. Experimental evaluation of the ELISE framework and the RL agent for four user requirement cases. In zone 1, the balanced user requirements is running ($\alpha = 0.4,\ \beta = 0.3,\ \gamma = 0.3$). Zone 2 depicts the case for the prioritized delay user requirements ($\alpha = 0.1,\ \beta = 0.8,\ \gamma = 0.1$). Zone 3 shows the case for the prioritized power consumption user requirements ($\alpha = 0.8,\ \beta = 0.1,\ \gamma = 0.1$), and zone 4 represents the case for the prioritized reliability user requirements ($\alpha = 0.1,\ \beta = 0.1,\ \gamma = 0.8$).

in the testbed and the limited size of observations impacting reliability. The average immediate reward is approximately 1.13 (Fig. 9d). The dispersion in network reliability affects the reward distribution, although not to the same extent as in the prioritized reliability case.

2) Prioritized delay: In this prioritized delay case, ELISE users assign higher priority to network delay compared to network reliability and power efficiency. The user coefficient values α, β, and γ are set to 0.1, 0.8, and 0.1, respectively. The prioritized delay requirement is activated after 40 timesteps and lasts for 40 timesteps (Zone 2 in Fig.9). The RL agent promptly adjusts to the new requirements, reducing the slotframe size from an average of 18 to 11 in approximately three actions. Due to the emphasis on delay, the network average delay is lower compared to other requirement cases. However, the network power consumption reaches its maximum as the slotframe size decreases. The network average delay, power consumption, and reliability are approximately 125ms, 4540μW, and 0.95, respectively (Fig.9b, Fig.9a, and Fig.9c). The average immediate reward is 1.13 and exhibits less variation compared to the previous case, reflecting the reduced contribution of network reliability in the reward function (Fig. 9d).

3) Prioritized power consumption: For the prioritized power consumption case, the emphasis is on network power efficiency rather than network delay and reliability. The user coefficient values α, β, and γ are set to 0.8, 0.1, and 0.1, respectively. The requirements for this case are activated after 80 timesteps and last for 40 timesteps (Zone 3 in Fig.9). The network transitions from a prioritized delay configuration to a prioritized power consumption configuration. The RL agent promptly detects the change in requirements (indicated by the immediate reward at timestep 80) and starts increasing the slotframe size. On average, the slotframe size increases from 11 to 34, taking around 13 actions to reach a steady state. As a result, the network experiences lower power consumption but higher delays overall. The network average delay, power consumption, and reliability are approximately 470ms, 4367μW, and 0.95, respectively (Fig.9b, Fig.9a, and Fig.9c). The average immediate reward is 1.14 and exhibits less variation compared to the balanced and reliable SDWSN cases, reflecting the reduced contribution of network reliability in the reward function (Fig. 9d).

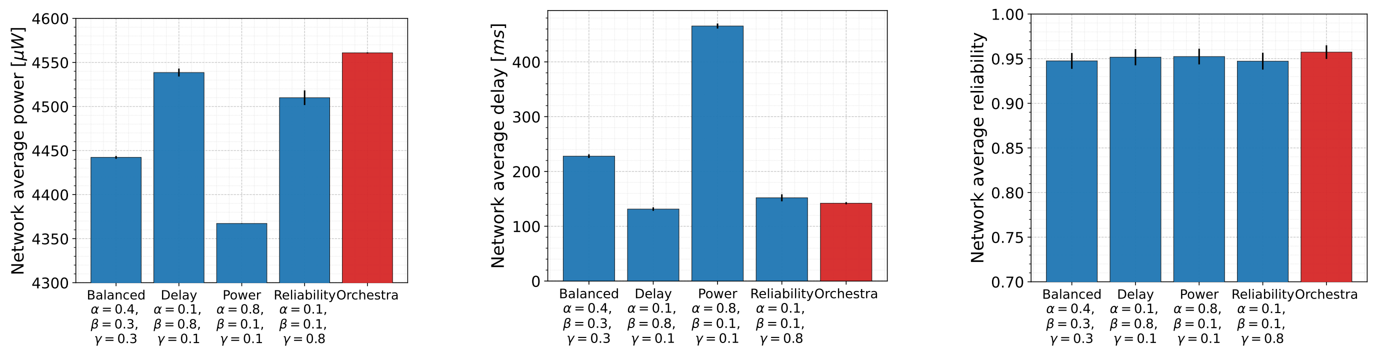

(a) Network average power consumption. (b) Network average delay. (c) Network average reliability.

Fig. 10. Experimental comparison between the ELISE framework and Orchestra.

4) Prioritized reliability: For the prioritized reliability case, the focus is on network reliability rather than network power consumption and delay. The weights selected for this case are $\alpha = 0.1$, $\beta = 0.1$, and $\gamma = 0.8$. The requirements are applied at timestep 120 and last for 40 timesteps (Zone 4 in Fig.9). At this point, the network transitions from a prioritized power consumption configuration to a prioritized reliability configuration. The RL agent detects the change in requirements and starts reducing the slotframe size. On average, it takes around 13 actions for the slotframe size to decrease to 12 and reach a steady state. Consequently, the network exhibits low delay (145ms in Fig.9b) and high power consumption (4510μW in Fig.9a). The network reliability remains high with an average steady-state value of 0.95 (Fig.9c). Overall, the network reliability is high for all user requirement cases, although it exhibits significant variation. This variation can be attributed to the frequency of TSCH schedule updates and the presence of multiple experiments and platforms in the densely populated testbed. The distribution of network reliability also impacts the immediate reward, but the RL agent successfully selects appropriate actions despite the noise (Fig. 9d).

5) ELISE and Orchestra: Fig. 10 compares the ELISE framework with Orchestra in terms of network power consumption, delay, and reliability. ELISE adapts the slotframe size to optimize power consumption, resulting in lower average power consumption compared to Orchestra. ELISE also achieves smaller average delays, while Orchestra's delay is similar to the prioritized delay scenario. In terms of network reliability, Orchestra performs slightly better than ELISE, likely due to its autonomous scheduling and fewer control packets transmitted.

VI. Conclusion and Future Work

We introduced ELISE, an open-source framework that utilizes deep reinforcement learning to optimize the slotframe size of TSCH for SDN-based IoT networks. ELISE effectively adapts network resources to dynamic user requirements and demonstrates its ability to maximize network performance. The framework encompasses various modules, including network management, data collection, schedule processing, route processing, and machine learning. Through experiments with different user requirements, ELISE showcases its ability to detect and respond to changes, achieving optimal performance.

However, the evaluation process reveals challenges in real-world deployments, such as the time-consuming training phase and occasional packet loss during network reconfigurations. To address these issues, future work will focus on improving training efficiency and minimizing reliability impacts. The ultimate goal is to develop an autonomous reinforcement learning scheduler within the ELISE framework that can adapt to user requirements seamlessly.

References

[1] F. Deng, X. Yue, X. Fan, S. Guan, Y. Xu, and J. Chen, "Multisource energy harvesting system for a wireless sensor network node in the field environment," *IEEE Internet of Things Journal*, vol. 6, no. 1, pp. 918–927, 2018.

[2] L. M. Borges, F. J. Velez, and A. S. Lebres, "Survey on the characterization and classification of wireless sensor network applications," *IEEE Communications Surveys & Tutorials*, vol. 16, no. 4, pp. 1860–1890, 2014.

[3] G. P. Joshi, S. Y. Nam, and S. W. Kim, "Cognitive radio wireless sensor networks: applications, challenges and research trends," *Sensors*, vol. 13, no. 9, pp. 11 196–11 228, 2013.

[4] S. M. Chowdhury and A. Hossain, "Different energy saving schemes in wireless sensor networks: A survey," *Wireless Personal Communications*, vol. 114, no. 3, pp. 2043–2062, 2020.

[5] D. Dujovne, T. Watteyne, X. Vilajosana, and P. Thubert, "6TiSCH: Deterministic IP-Enabled Industrial Internet (of Things)," *IEEE Communications Magazine*, vol. 52, no. 12, pp. 36–41, 2014.

[6] Y. Ha and S.-H. Chung, "Traffic-aware 6TiSCH Routing Method for IIoT Wireless Networks," *IEEE Internet of Things Journal*, 2022.

[7] F. F. Jurado-Lasso, L. Marchegiani, J. F. Jurado, A. M. Abu-Mahfouz, and X. Fafoutis, "A survey on Machine Learning Software-Defined Wireless Sensor Networks (ML-SDWSNs): Current status and major challenges," *IEEE Access*, vol. 10, pp. 23 560–23 592, 2022.

[8] S. Bera, S. Misra, and A. V. Vasilakos, "Software-defined networking for internet of things: A survey," *IEEE Internet of Things Journal*, vol. 4, no. 6, pp. 1994–2008, 2017.

[9] H. I. Kobo, A. M. Abu-Mahfouz, and G. P. Hancke, "A survey on software-defined wireless sensor networks: Challenges and design requirements," *IEEE access*, vol. 5, pp. 1872–1899, 2017.

[10] S. Duquennoy, B. Al Nahas, O. Landsiedel, and T. Watteyne, "Orchestra: Robust mesh networks through autonomously scheduled TSCH," in *Proceedings of the 13th ACM conference on embedded networked sensor systems*, 2015, pp. 337–350.

[11] M. R. Palattella, N. Accettura, L. A. Grieco, G. Boggia, M. Dohler, and T. Engel, "On optimal scheduling in duty-cycled industrial IoT applications using IEEE802. 15.4 e TSCH," *IEEE Sensors Journal*, vol. 13, no. 10, pp. 3655–3666, 2013.

[12] T. Watteyne, M. Palattella, and L. Grieco, "Using IEEE 802.15. 4e Time-Slotted Channel Hopping (TSCH) in the Internet of Things (IoT): Problem statement," Tech. Rep., 2015.

[13] V. Kotsiou, G. Z. Papadopoulos, P. Chatzimisios, and F. Theoleyre, "LDSF: Low-latency Distributed Scheduling Function for Industrial Internet of Things," *IEEE Internet of Things Journal*, vol. 7, no. 9, pp. 8688–8699, 2020.

[14] S. Misra, S. Bera, M. P. Achuthananda, S. K. Pal, and M. S. Obaidat, "Situation-Aware Protocol Switching in Software-Defined Wireless Sensor Network Systems," *IEEE Systems Journal*, vol. 12, no. 3, pp. 2353–2360, 2017.

[15] L. L. Bello, A. Lombardo, S. Milardo, G. Patti, and M. Reno, "Experimental assessments and analysis of an SDN framework to integrate mobility management in industrial wireless sensor networks," *IEEE Transactions on Industrial Informatics*, vol. 16, no. 8, pp. 5586–5595, 2020.

[16] T. Theodorou and L. Mamatas, "SD-MIoT: A Software-Defined Networking Solution for Mobile Internet of Things," *IEEE Internet of Things Journal*, vol. 8, no. 6, pp. 4604–4617, 2020.

[17] T. G. Nguyen, T. V. Phan, D. T. Hoang, T. N. Nguyen, and C. So-In, "Federated Deep Reinforcement Learning for Traffic Monitoring in SDN-Based IoT Networks," *IEEE Transactions on Cognitive Communications and Networking*, vol. 7, no. 4, pp. 1048–1065, 2021.

[18] M. U. Younus, M. K. Khan, and A. R. Bhatti, "Improving the Software-Defined Wireless Sensor Networks Routing Performance Using Reinforcement Learning," *IEEE Internet of Things Journal*, vol. 9, no. 5, pp. 3495–3508, 2021.

[19] H. Hajizadeh, M. Nabi, and K. Goossens, "Decentralized Configuration of TSCH-Based IoT Networks for Distinctive QoS: A Deep Reinforcement Learning Approach," *IEEE Internet of Things Journal*, 2023.

[20] G. Oikonomou, S. Duquennoy, A. Elsts, J. Eriksson, Y. Tanaka, and N. Tsiftes, "The Contiki-NG open source operating system for next generation IoT devices," *SoftwareX*, vol. 18, p. 101089, 2022.

[21] F. Osterlind, A. Dunkels, J. Eriksson, N. Finne, and T. Voigt, "Cross-Level Sensor Network Simulation with Cooja," in *Proceedings. 2006 31st IEEE conference on local computer networks*. IEEE, 2006, pp. 641–648.

[22] M. Pilgrim and S. Willison, *Dive into python 3*. Springer, 2009, vol. 2.

[23] N. C. Luong, D. T. Hoang, S. Gong, D. Niyato, P. Wang, Y.-C. Liang, and D. I. Kim, "Applications of deep reinforcement learning in communications and networking: A survey," *IEEE Communications Surveys & Tutorials*, vol. 21, no. 4, pp. 3133–3174, 2019.

[24] V. Mnih, A. P. Badia, M. Mirza, A. Graves, T. Lillicrap, T. Harley, D. Silver, and K. Kavukcuoglu, "Asynchronous methods for deep reinforcement learning," in *International conference on machine learning*. PMLR, 2016, pp. 1928–1937.

[25] J. Schulman, F. Wolski, P. Dhariwal, A. Radford, and O. Klimov, "Proximal policy optimization algorithms," *arXiv preprint arXiv:1707.06347*, 2017.

[26] C. Adjih, E. Baccelli, E. Fleury, G. Harter, N. Mitton, T. Noel, R. Pissard-Gibollet, F. Saint-Marcel, G. Schreiner, and J. Vandaele, "FIT IoT-LAB: A large scale open experimental IoT testbed," in *2015 IEEE 2nd World Forum on Internet of Things (WF-IoT)*. IEEE, 2015, pp. 459–464.

[27] A. Raffin, A. Hill, A. Gleave, A. Kanervisto, M. Ernestus, and N. Dormann, "Stable-baselines3: Reliable reinforcement learning implementations," *Journal of Machine Learning Research*, 2021.

[28] T. Akiba, S. Sano, T. Yanase, T. Ohta, and M. Koyama, "Optuna: A next-generation hyperparameter optimization framework," in *Proceedings of the 25th ACM SIGKDD international conference on knowledge discovery & data mining*, 2019, pp. 2623–2631.

F. Fernando Jurado-Lasso (GS'18-M'21) received the Ph.D. degree in Engineering and the M.Eng. degree in Telecommunications Engineering both from The University of Melbourne, Melbourne, VIC, Australia, in 2020 and 2015, respectively; a B.Eng. degree in Electronics Engineering in 2012 from the Universidad del Valle, Cali, Colombia. He is currently a postdoctoral researcher at the Embedded Systems Engineering (ESE) section of the Department of Applied Mathematics and Computer Science of the Technical University of Denmark (DTU Compute).

His research interests include networked embedded systems, software-defined wireless sensor networks, machine learning, protocols and applications for the Internet of Things.

Mohammadreza Barzegaran has been a postdoctoral research fellow in computer science at the Technical University of Denmark since 2021. His research is focused on the configuration of Fog computing platform for critical control applications. His main research interests concern Fog/Edge computing, optimization, the configuration of real-time and safety-critical systems, and co-design of control applications for real-time and safety-critical systems

J. F. Jurado received the Doctorate and MSc degree in Physics both from Universidad del Valle, Cali, Colombia, in 2000 and 1986, respectively; he also holds a BSc degree in Physics from the Universidad de Nariño, Pasto, Colombia in 1984.

He is currently a Professor with the Faculty of Engineering and Administration of the Department of Basic Science of The Universidad Nacional de Colombia Sede Palmira, Colombia. His research interests include nanomaterials, magnetic and ionic materials, nanoelectronics, embedded systems and the Internet of Things. He is a senior member of Minciencias in Colombia.

Xenofon Fafoutis (S'09-M'14-SM'20) received a PhD degree in Embedded Systems Engineering from the Technical University of Denmark in 2014; an MSc degree in Computer Science from the University of Crete (Greece) in 2010; and a BSc in Informatics and Telecommunications from the University of Athens (Greece) in 2007. From 2014 to 2018, he held various researcher positions at the University of Bristol (UK), and he was a core member of SPHERE: UK's flagship Interdisciplinary Research Collaboration on Healthcare Technology. He is currently an Associate Professor with the Embedded Systems Engineering (ESE) section of the Department of Applied Mathematics and Computer Science of the Technical University of Denmark (DTU Compute). His research interests primarily lie in Wireless Embedded Systems as an enabling technology for Digital Health, Smart Cities, and the (Industrial) Internet of Things (IoT).